Computers and Electrical Engineering 96 (2021) 107480

Contents lists available at ScienceDirect

Computers and Electrical Engineering

journal homepage: www.elsevier.com/locate/compeleceng

Prediction of wind farm reactive power fast variations by adaptive one-dimensional convolutional neural network☆

Haidar Samet [a,b,*], Saeedeh Ketabipour [a], Shahabodin Afrasiabi [c], Mousa Afrasiabi [a], Mohammad Mohammadi [a]

[a] School of Electrical and Computer Engineering, Shiraz University, Shiraz, Iran
[b] Department of Electrical Engineering, Eindhoven University of Technology, Eindhoven, the Netherlands
[c] Department of Electrical and Computer Engineering, University of Saskatchewan, Saskatoon, Canada

ARTICLE INFO

Editor: Dr. M. Malek

Keywords:
Wind energy
Flicker emission
Deep neural network
One dimensional convolutional deep learning network
Static VAr compensator
Wind farm

ABSTRACT

One of the prominent problems in wind farms is voltage flicker emission. To prevent flicker emission or mitigate the impact as best as possible, a static VAr compensator (SVC) is a great candidate both economically and technically. However, SVCs cannot completely compensate the fast-changing reactive power due to delays caused by the reactive power calculation unit and the triggering fire angle of the SVC. This paper proposes a predictive control system for SVCs, by merging an additional predictive control block into the conventional control system. It is constructed based on deep neural networks, namely adaptive one-dimensional convolutional neural network (1D-CNN). The training process is conducted based on the adaptive learning weights process to enhance the prediction accuracy and training computational complexity of the 1D-CNN. Numerical results on the actual dataset in a wind farm in Manjil, Iran, have verified the forecasting accuracy and flicker mitigation of the proposed controller.

1. Introduction

1.1. Motivation

Wind energy has become an impartible part of sustainable energies in today's world. The rapid development of sustainable technologies has led to a high growth rate of wind energy conversion systems in the last decade [1], where more than 600 GW of electrical energy was supplied worldwide at the end of 2018, with the potential generation being approximately 1280 TWh. The major challenge in the development of wind turbines is the inherent intermittency of wind energy, this can lead to several problems in the reliability, high maintenance, and especially in the power quality of electrical networks. Wind speed variation could cause voltage fluctuation in terms of flicker phenomenon in connection point of wind turbine and electric grid. Flicker is generally defined as a low-frequency voltage fluctuation from between 10%-90% in the predefined frequency range (0.005 to 35 Hz) [2]. Flicker emission is significantly increased in the grid-connected wind farm due to the variation in metrological data such as wind speed and failures of electronic and mechanical components of the wind turbines. Moreover, wind farms are generally located in far areas from the cities, in

☆ This paper is for special section VSI-aisg. Reviews processed by the Editor-in-Chief Dr. Manu Malek.

* Corresponding author.
E-mail addresses: samet@shirazu.ac.ir, h.samet@tue.nl (H. Samet).

https://doi.org/10.1016/j.compeleceng.2021.107480
Received 3 June 2020; Received in revised form 27 August 2021; Accepted 22 September 2021
Available online 12 October 2021

sensitive places in terms of frequency and voltage stability, which does not support the flicker problem.

In order to mitigate flicker emission, static VAr compensator (SVC) has been considered the main device in terms of economy and technical consideration [3]. However, the major disadvantage of the SVC is an inherent delay due to switching limitations caused by thyristor ignition delay [4]. In this study, we aim to resolve this problem using a predictive structure based on real-time deep learning techniques to provide prior knowledge in next time steps and compensate for the SVC delay.

1.2. Brief literature review

There are two main groups of methods that have been presented in order to alleviate the flicker emission in the previously presented literature. In the first group of the presented methods, the modified/advanced control systems are presented for a specific wind turbine structures, while in the second group of methods, an auxiliary device such as the reactive power compensator e.g. flexible AC transmission system (FACTS) is installed to enhance the performance of the wind turbines.

To address negative potential impacts of the power quality disturbance, including flicker fluctuations, a reconfiguration of the control system has been proposed in the previous investigations. For instance, a control system in [5] for smart load control is presented to reduce flicker mitigation, which is situated between the wind farm and the main grid. A control system based on injected power (active/reactive) by wind turbines equipped by doubly-fed induction generators (DFIG) to the grid is presented in [6]. In [7], an intelligent control system based on the fuzzy logic is presented for a wind turbine connected to a permanent magnet synchronous generator (PMSG). It is undeniable that the generality of this type of method is questionable and modifications of the control system are only applicable to a specific wind farm. However, in order to apply the first type of method, it is essential to equip the grid-connected wind farms with high-tech infrastructures such as power electronic devices, which are highly expensive in terms of maintenance and their purchasing prices.

In the second type of method, reactive power compensation devices are implemented in point of coupling connection (PCC) to support wind farms in mitigating the flicker emission. To regulate the voltage fluctuation, FACTS has gained high attention in recent years [2]. To address the reactive power compensation, static VAr controller (SVC) and static synchronous compensator (STACOM) are the potential FACTS that can play a role in the power quality improvement in terms of voltage flicker [8]. From an economic perspective, SVC has been considered as a cost-effective reactive compensator in the aims of improving power quality disturbances, especially flicker emission reduction [2]. Despite these advantages, SVC struggles with a major challenge caused by switching limitations, which leads to a time delay (about half-cycle). The switching limitation in SVC arises from the thyristor ignition delay. To compensate this delay and tackle this huge challenge in the operation of the SVC in grid-connected wind farms, extremely short-term forecasting methods can be a potential solution. In a better word, the predicted values for one half-cycle ahead are replaced with values at current time. Although using prediction of instantaneous reactive power seems to be a potential tool to avoid the inherent time delay of the SVCs, the forecasting method should be able to estimate the reactive power in a look-ahead times with a low level of error.

Based on time periods, wind speed/power forecasting methods are classified in Table 1 to five categories; extremely short [2] and [4], very short [9], short [10], medium [13], and long [14] prediction horizon. The first group of this division is long-term forecasting methods, which usually include forecasting from one day to one week ahead and more. Long-term forecasting is used in optimal planning problems and finding optimal decision variables in the power operational problems. The second group contains forecasting methods in the mid-term, which consists of the prediction of six hours to two days ahead. Medium-term forecasting is applicable in the day-ahead decision making problems. The third group is short-term prediction methods with a time horizon in the range of [30min, 6hr]. Some applications of the short-term prediction are economic load dispatch planning, load increment/decrement decisions. The fourth group of this division is very short-term forecasting methods, which includes the forecasting method with a time horizon in the range of seconds to 30 minutes and it is essential in electricity market analysis studies.

The fifth group is regarding extremely short term modeling and forecasting methods for wind power of time samples less than one cycle (0.02 s). Extremely short time modeling of active and reactive powers variations is essential for modeling power quality issues. As mentioned previously, extremely short-forecasting is a basic principle of the proposed controller system to improve the SVC performance. However, extremely short-term wind power prediction is considered only in [2] and [4] and there is no other studies in this category.

In terms of forecasting models, five main categories are previously presented in the literature [10] including persistence, physical, statistical, artificial, and hybrid methods. The persistence, physical, and statistical models are suffered from disability in capturing non-stationary and complex features of a time series (persistence and statistical models) [15] and high computational burden (physical models), which make them more or less an inappropriate candidate for extremely short-term reactive power forecasting. Artificial intelligent (AI) based forecasting techniques take advantage of the ability to understand the highly time-variant sequences. The

Table 1
Wind power prediction categories: prediction time horizon.

Prediction horizon	Time interval	References
Extremely short	t$\leq 0.02s$	Only [2] and [4]
Very short	$1s \leq t \leq 30min$	[9]
Short	$30min \leq t \leq 6hr$	[10, 11], and [12]
Medium	$6hr \leq t \leq 24hr$	[13]
Long	$1day \leq t \leq 7days$	[14]

AI-based methods attempt to learn features from time-series data. In general, AI-based methods can be categorized into [11]: i) shallow, ii) deep, while shallow-based structures suffer from the disability to handle an extreme short-term time series as reactive power. Therefore, shallow-based methods are regularly merged into an additional feature extraction, such as spectral analysis techniques, discrimination power analysis (DPA) [16,17], and present as hybrid techniques. Hybrid techniques might have revealed a proper performance in some cases, whereas they are computationally expensive, highly sensitive to noises as well as lacking generality to different types of datasets. Moreover, shallow-based techniques, regardless of whether they are supplied with raw data or not, are restricted to the small number of learning parameters [18]. To address these problems, deep learning has presented significant performance in automatically learn features from raw data and the potential capability to handle an extreme short-term time series [1].

1.3. Contributions and organization

In this paper, deep learning is selected as a potential candidate to integrate into an SVC control system to resolve the time-delay problem and therefore, propose a predictive control structure and improve the performance of the grid-connected wind farms. Convolutional neural networks (CNNs) are special deep networks and strong learners from raw data, in particular in time series forecasting problems [1]. CNN has far fewer parameters in comparison with other deep networks and therefore, requires less memory space. In addition, the convolution operator makes that CNN a great inherent feature extractor. However, a common CNN is well designed for two-dimensional (2D) data and it requires a dataset of labeled 2D data [19], which makes 2D-CNN unsuitable for real-time applications. There are several issues that make 1D-CNN advantageous and thus preferable to 2D-CNN for application in the real-time control system of SVCs: i) lower computational complexity, ii) easy implementation and training, and iii) lower-cost hardware for the practical implementation.

Therefore, we design a 1D-CNN structure for the instantaneous reactive power prediction. The major difference is the utilization of 1D-convolutional layers instead of 2D layers, and thereby reduce computational complexity and make it a feasible and inexpensive alternative for applying in the proposed predictive controller for SVCs. Furthermore, to generalize a proposed method, the wind farm is modeled as a time-variant current source that the phasor values changed in an extremely time period (at ms level with 50 Hz frequency). To mimic a real condition, as best as possible, the actual wind farm active and reactive power data are recorded in an actual wind farm in Manjil, Iran. To verify the effectiveness of the proposed 1D-CNN based predictive controller, the proposed structure

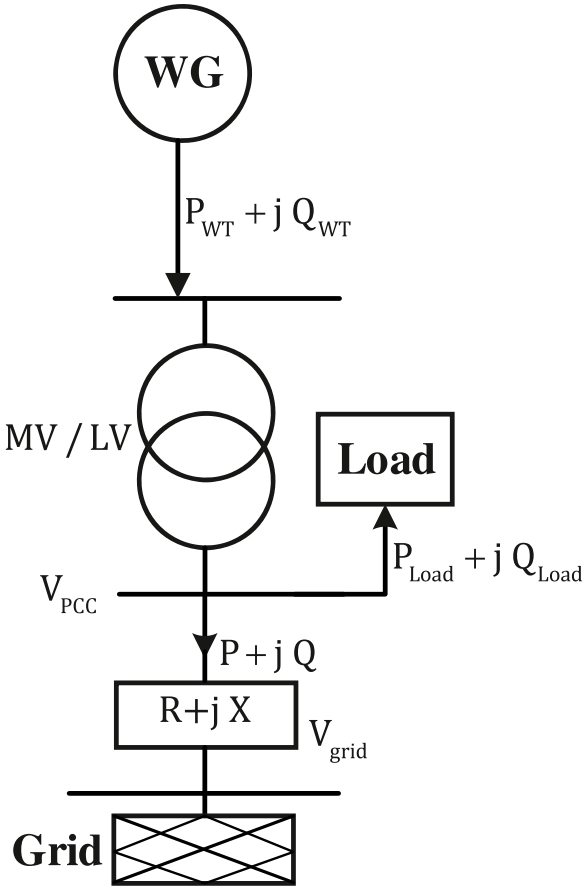

Fig. 1. A general diagram for a wind farm.

performance in flicker impact mitigation is compared in different cases. The numerical results have verified the effectiveness of the proposed method based on flicker sensation measures.

The main novelties of the current work are enumerated, as:

(1) This paper designs an adaptive 1D-CNN based extremely short-term forecasting for the instantaneous reactive power of wind generations that can perform accurately as well as computationally efficient. In previous works, there are several previously presented works on short/medium/long prediction. However, extremely short-term forecasting is rarely investigated in previous studies (i.e. [2] and [4]). The proposed method solves the problems including the high computational complexity, unable to modeling nonlinear and complex structures, and a requirement to 2D labeling.
(2) To speed up the training process and enhance the accuracy as well as reliability of the proposed deep-based predictive block, an adaptive training process is proposed to integrate into the conventional 1D-CNN, and thereby, the extremely short-term prediction accuracy has significantly improved.
(3) In contrast with the previous works that only work on the simulation data, to mimic real conditions, as best as possible, we establish a large-scale reactive power dataset in a large-scale wind farm in Manjil, north of Iran, with an extremely short time horizon (ms).

The organization of this paper is as follows: In Section II, the background of the predictive controller for SVC is presented. In Section III, the proposed adaptive 1D-CNN is provided. Section IV describes the application of adaptive 1D-CNN for SVC controller. Section V gives the discussion on the results based on the actual data of a wind farm in Manjil, Iran.

2. Background of predictive controller for SVC

This section briefly introduces the principle of the proposed extremely short-term forecasting control system for the SVCs in large-scale wind farms. Fig. 1 depicts a general form for a wind farm.

The amplitude of voltage and corresponding angles are highly influenced by inherent intermittency of wind speed, therefore, voltage at PCC is obtained as:

$$V_{PCC} = V_{grid} + I(R + j\,X) \tag{1}$$

where V_{PCC}, V_{grid}, and I demonstrate voltage at the PCC, voltage at the MV/LV transformer, and is the current of line between PCC and grid, while R and Xrepresent resistor and reactance of the line. According to reference value of voltage at the PCC, V_{PCC}^{ref}, V_{PCC} is obtained based on line power flow P and Q can be rewritten as:

$$V_{PCC} = V_{grid} + \frac{P - jQ}{V_{PCC}^{ref}}(R + j\,X) \tag{2}$$

Therefore, voltage amplitude variation is obtained based on electrical power (active and reactive) is given as [20]:

$$\Delta V = \Delta V_R + j\,\Delta V_X = \frac{PR + QX}{V_{PCC}^{ref}}(R + j\,X) \tag{3}$$

The voltage angle between the voltage at the PCC and voltage at the MV/HV substation is typically small, while voltage amplitude is adversely changing, which is determined by the first term in (3), $\frac{PR+QX}{V_{PCC}^{ref}}$. Voltage variation can be rewritten as a function of active power variation ΔP and reactive power variationΔQ, respectively, and:

$$\Delta|V| = |V_{PCC}| - |V_{grid}| = \frac{PR + QX}{V_{PCC}^{ref}}(R + j\,X) \tag{4}$$

To regulate voltage fluctuation, unity power factor is preferred and therefore voltage variation is obtained by ignoring the resistance values at the PCC, as:

$$\Delta|V_{PCC}| \approx \frac{1}{V_{PCC}^{ref}}(\Delta Q \cdot X) \tag{5}$$

To eliminate, or at least mitigate, the voltage variation, three general alternatives would be available for the operators, including: i) expansion the electrical networks and installation of new devices including lines and local generators or reconfiguration of the power systems, ii) developing the control system using advanced devices, and iii) installation of FACTS devices such as the SVC to adjust reactive power and enhance the power quality. Since the reactive power compensators are far more adaptive with all types of wind turbines, FACTS devices such as SVC is preferred. Furthermore, FACTS devices can regulate the voltage and significantly restrict voltage variations, even might keep it constant.

In general, the control system of the SVCs consists of a feedback loop and a feedforward loop. In the feedback loop, a PI-controller adjusts the reactive power at the grid bus, while the feedforward loop regulates the output reactive of the wind farm. Then, a reference value for thyristor firing angle adjustment is determined to adjust reactive power. However, a half-cycle delay time of the feed forward loop adversely affects the performance of SVC.

To address this problem, a forecasting engine is added to the feedforward loop. The proposed predictive controller for SVC is presented in Fig. 2.

The feedback controller, similar to the conventional controller of SVC, is fed by the electric grid based on the measured currents and voltage by the current transformer (CT) and power transformer (PT), respectively. The instantaneous current and voltage are used to compute the instantaneous reactive power and then set as an input to the PI-controller. This loop adjusts the state error and so on, the average value of reactive power to zero. The feedback block is dynamically slower and the delay is about 200 ms.

To mitigate voltage flicker, the feedforward loop is utilized to compensate for the reactive power alteration and thereby mitigation of voltage flicker. This loop performs faster than the conventional block in terms of dynamic response within a delay (half-cycle) and uses recorded actual data of wind farms in a control system to determine the reactive power values supplying by SVC. In this paper, we proposed an adaptive 1D CNN-based for reactive power prediction in an extremely short time horizon to tackle the problem associated with low-speed dynamic response and thyristor firing delay. Hence, the extremely short-term forecasting block improves the reactive power compensation process and prohibits the time delay and associated restriction for the control system bandwidth.

3. Adaptive 1D-CNN based extremely short-term forecasting block

To address the proposed adaptive 1D-CNN based reactive power prediction, this section provides required explanations. CNN is a powerful feature extraction deep structure, which benefits from sparse connection and weight sharing. CNN does not need a large number of parameters in comparison with other deep networks due to weight sharing, and the weight sharing technique enhances the computational efficiency. This paper draws on the application of the designed adaptive 1D-CNN in the extremely short-term prediction of reactive power within a half-cycle time interval. The designed adaptive 1D-CNN model needs an input data preparation process, and consists of three main sets of layers, i.e. convolution, pooling, and fully-connected networks (FCN) layers. In the next subsections, each major block of the designed adaptive 1D-CNN is described.

3.1. Input data preparation

The actual recorded reactive power time series is originally in 1D form. Therefore, only a half-cycle of the recorded actual data is segmented as:

$$Q_s = \left[Q_{WT}^1,\ Q_{WT}^2, \cdots, Q_{WT}^k\right] \tag{6}$$

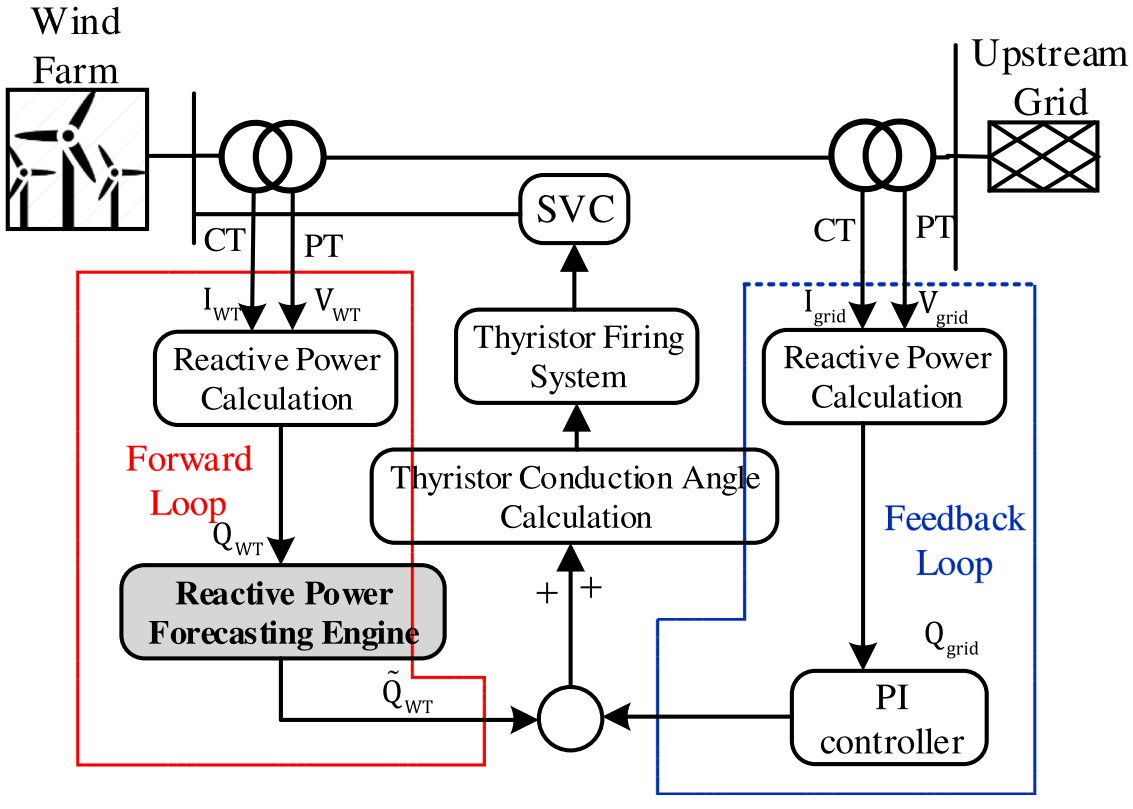

Fig. 2. Principle of the predictive controller for SVC connected in parallel with a wind farm.

where Q_s indicates a set of the k different samples of the reactive power generated by the wind farms Q_{WT}, which is used for training and testing process.

3.2. Convolutional layers

The raw time series of reactive power from the input dataset is received, and the number of convolution kernels in each convolution layer is used as the first inherent feature extraction. To this end, features from one-dimension inputs are extracted by convolutional operators to train a network consist of multiple kernels and weights [21,22].

3.3. Max-pooling layers

The pooling layers are typically used to scale and project data from the upper layers to reduce dimensions through overlapping convolution windows and moreover contribute to capturing features.

3.4. Fully-connected layers

The fully-connected layers in the designed adaptive 1D-CNN are applied to provide a connection between layers in CNN, regulation of the designed adaptive deep network, and construct the predicted values.

3.5. Proposed adaptive training

The actual recorded data is normalized in specific time intervals (10 ms). To train and evaluate the adaptive 1D-CNN, the actual data is decomposed into test/train subsets. The adaptive deep learning method is trained for applying in real-time forecasting, while the testing subset is used to evaluate the performance.

In the training process, firstly, the initial values of the hyper-parameters including the number of the layers l, the number of hidden states u, and batch sizes bs of each layer in the designed 1D-CNN network are determined. To this end, a loss function is defined, which is mean absolute percentage error (MAPE), as:

$$f_{loss} = \frac{1}{bs}\frac{1}{O}\sum_{x=1}^{bs}\sum_{y=1}^{O}\left|\frac{\overline{Q}_{WT} - Q_{WT}}{Q_{WT}}\right| \tag{7}$$

where O indicates the output time series size. This loss function is the core of the learning process in a repetitive manner.

Then, back-propagation process is used to find the learning weights as:

$$\mathscr{G} = \frac{\partial f_{loss}}{\partial \omega_{mn}^{l}} = \sum_{\alpha\beta}\rho_n^l(\alpha\beta)\left(y_n^{l-1}\omega_{mn}^{l}\right) \tag{8}$$

where $\mathscr{G}$, ω_{mn}^{l}, and $\rho_n^l(\alpha\beta)$ represent the set of gradient weights, learning weights where connect the m^{th} feature map of the l^{th} layer to n^{th} feature map of the previous layer, $l-1$, and sensitivity of neurons α and β, respectively. The loss function is modified based on the sparse connection weights, as:

$$f_{loss}^{'} = f_{loss} + \sum_{\alpha\beta}|\vartheta(\alpha\beta)| \tag{9}$$

Thus, gradient weights are computed as:

$$\mathscr{G} = \frac{\partial f_{loss}^{'}}{\partial \omega_{mn}^{l}} = \frac{\partial f_{loss}}{\partial \omega_{mn}^{l}} + \frac{\partial \vartheta(\alpha\beta)}{\partial \omega_{mn}^{l}} \tag{10}$$

To optimize the loss function and find the optimal learning weights, generally, the learning weights are considered a constant. The constant learning weight in the training of the dataset can increase the loss error and poor performance in the time series prediction. Contrarily, the low rate can overcome this problem by significantly increasing the computational time. To tackle this problem, this paper proposes an adaptive training process to upgrade learning weights ω_{mn}^{l}. To this end, κ and τ are defined:

$$\kappa = \begin{cases} 1 & if \;\; f^s\left(\mathscr{G}_{mn}^{tr}\mathscr{G}_{mn}^{tr-1}\right) = 1 \\ -1 & if \;\; f^s\left(\mathscr{G}_{mn}^{tr}\mathscr{G}_{mn}^{tr-1}\right) = 0 \end{cases} \tag{11}$$

$$\tau^{tr} = c^{\kappa}\tau^{tr-1} \tag{12}$$

where $\mathscr{G}_{mn}^{tr}$ indicates the gradient weights at tr training, while c^{κ} and τ^{tr} are regulation variables. Furthermore, $f^s(\bullet)$ represents the function to determine the gradients weights orientation. To minimize the loss function in the training process and lead to the optimal learning weights and speed up convergence, κ should be fall into [0, 1], therefore, c^{κ} be between the [0, 1] or [1, 2]. In the proposed

adaptive training process, adding momentum term τ^{tr} prevents slow condition and regulates the learning weights during the training. Thus, the learning weights are upgraded as follows:

$$\omega_{mn}^{tr} = \omega_{mn}^{tr-1} - \tau^{tr}(1-\zeta)\frac{\partial f_{loss}}{\partial \omega_{mn}^{tr}} - \tau^{tr}\zeta\frac{\partial f_{loss}}{\partial \omega_{mn}^{tr-1}} \tag{13}$$

where ζindicates a regulation parameter between [0, 1] and values are depend on the last two training process.

To enhance the computational efficiency and reduce the possibility of overfitting the designed adaptive CNN, network a technique, namely dropout technique is used.

Furthermore, the activation function in almost all layers is rectified linear unit (ReLU), while linear activation function is used in the last FCN layer. Additionally, to set the hyperparameters of the designed adaptive deep network, the root mean square propagation (RMSProp) has been adopted from [23] to find the optimal values for hyperparameters.

4. Application of adaptive 1D-CNN for SVC controller

To illustrate the generality of the proposed method, the wind farm I considered as a variable current source. In this wind farm model, the magnitude and phases of the three-phase currents are upgraded at each 10 ms (depend on nominal frequency, 50 Hz). The wind farm model and the proposed predictive controller based on adaptive 1D-CNN are displayed in Fig. 3.

The currents and phases are updated at each *k*-th half-cycle by solving (14–15) for every half cycle. Eqs. (14-15) simply can be attained by applying active and reactive powers balance in Fig. 4.

$$P_k = -R_{Th}I_k^2 + V_{Th}I_k\ cos(\alpha_k) \tag{14}$$

$$Q_k = -X_{Th}I_k^2 - V_{Th}I_k\ sin(\alpha_k) \tag{15}$$

The output active and reactive power of the wind farm is represented by $P_k$and Q_k at k^{th} time interval, respectively. Furthermore, Thevenin circuit values including voltage, resistance, and reactance are presented by V_{Th}, R_{Th}, and X_{Th}, respectively.

By summing square of (14) and (15), the resulted equation will be as follows:

$$aI_k^4 + bI_k^2 + c = 0 \tag{16}$$

where:

$$a = R_{Th}^2 + X_{Th}^2 \tag{17}$$

$$b = 2P_kR_{Th} + 2X_{Th}Q_k - V_{Th}^2 \tag{18}$$

$$c = P_k^2 + Q_k^2 \tag{19}$$

In (16), there are two positive roots. Based on the actual records, the smaller root is the answer which is calculated as:

$$I_k^2 = \frac{-b - \sqrt{b^2 - 4ac}}{2a} \tag{20}$$

Then I_k is calculated as the square root of the positive answer in (20).

Now α_k simply can be calculated by (21):

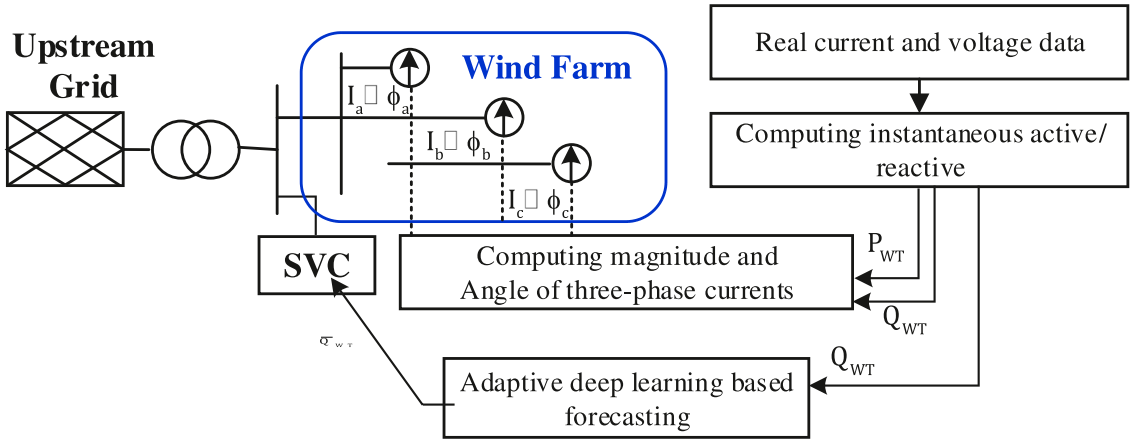

Fig. 3. Wind farm model and adaptive 1D-CNN based control system.

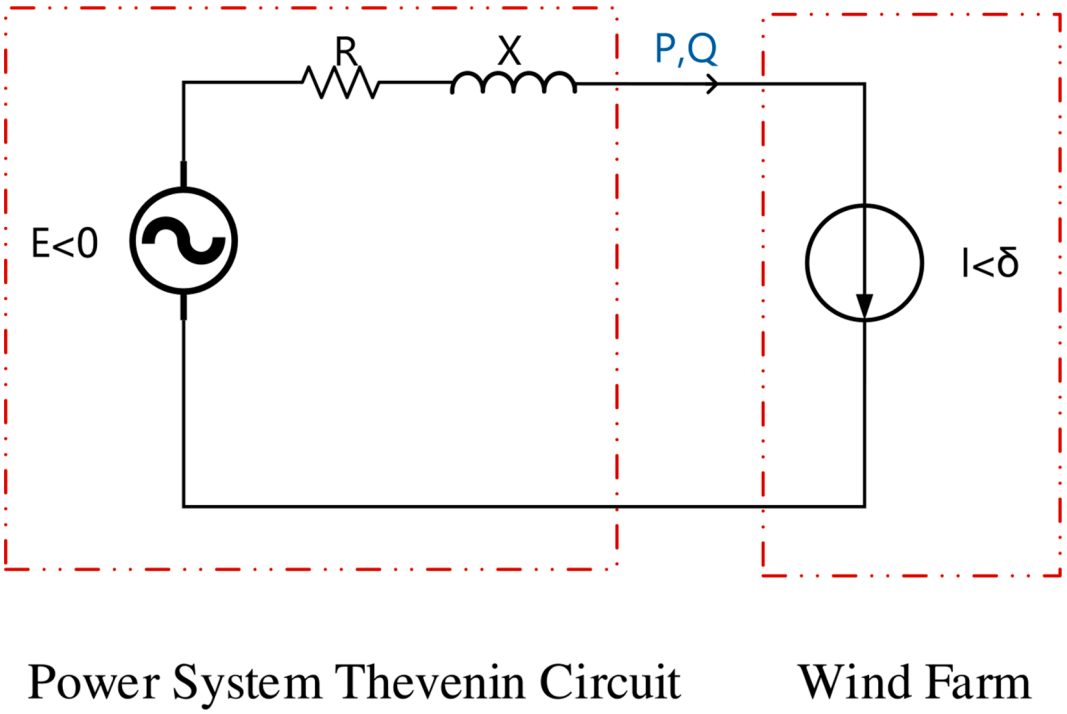

Fig. 4. A simple circuit regarding to Eq. (12).

$$\alpha_k = cos^{-1}\left(\frac{P_k + R_{Th}I_k^2}{V_{Th}I_k}\right) \tag{21}$$

To compensate for the time delay caused by the internal structure of the SVC, the designed 1D-CNN structure is applied, which is illustrated and visualized in Figure 5 and Figure 6, respectively. To implement, adaptive 1D-CNN for the real-time reactive power forecasting, as follows:

1 The actual recorded data is firstly normalized and then formed as a set of tensors with dimension $S \times 128 \times 1$ (S stands for sample).
2 As illustrated in Fig. 5, the raw instantaneous reactive power is fed into the first one-dimensional convolutional layer, presented by Conv 1 in Fig. 5. This layer converts the input dataset into the feature vector with $S \times 128 \times 2$ size.
3 In this paper, max pooling layers are selected to pool generated feature maps in the convolutional layers through a maximization of generated feature maps over each time interval and outputs a set of vectors with $S \times 128 \times 2$ dimension.
4 The output of pooling layers is the input of the second convolutional layer, namely Conv 2, with 10% dropout probability and then generates the output with $S \times 128 \times 2$.
5 Then, the output of Conv 2 has considered as the input of the first fully-connected layer. However, the input of fully-connected layers firstly should be flattened, then fed into the first fully connected layers and formed a set of output with $S \times 128 \times 1$.
6 The output of the first fully-connected layers is considered as the input of the second fully connected layers. The outputs of second fully-connected layers are formed as the feature vectors with S × 64 (64 is the number of hidden units).
7 Consequently, the predicated reactive power is constructed for a specific time interval (half-cycle).

Note: In the CNN-based networks, the output of convolutional layer is determined by $Output_{Size} = \frac{input_{size} - kernel_{size} + 2\times padding}{Stride} + 1$. Considering $input_{size} = 56$ (number of samples at each half-cycle of data), $kernel_{size} = 55$, $padding = 0$, and $Stride = 1$, output of first convolutional layer is, $\frac{(56-55+2\times 0)}{1} + 1 = 2$. The number of filters has been considered as 128. Thus, the output of Conv 1 is the feature vector with dimension$S \times 128 \times 2$. Furthermore, The output of max-pooling is determined by $Output_{Size} = \frac{input_{size} - pool_{size} + 2\times padding}{Stride} + 1$, considering$padding = 1$, $Stride = 2$, and $pool_{size} = 2$. Then, $\frac{2-2+2\times 1}{2} + 1 = 2$. The number of filters is 128. Thus, the output of max-poling is the feature vector with dimension $S \times 128 \times 2$.

5. Numerical results

In this section, the proposed forecasting engine for an extremely short time period and enhancing the control system performance of the SVCs connected to wind farms are investigated. Thus, firstly, experimental data is briefly described. Then, the performance of the proposed adaptive 1D-CNN is discussed and compared with other methods in terms of accuracy. Then, the application of the proposed

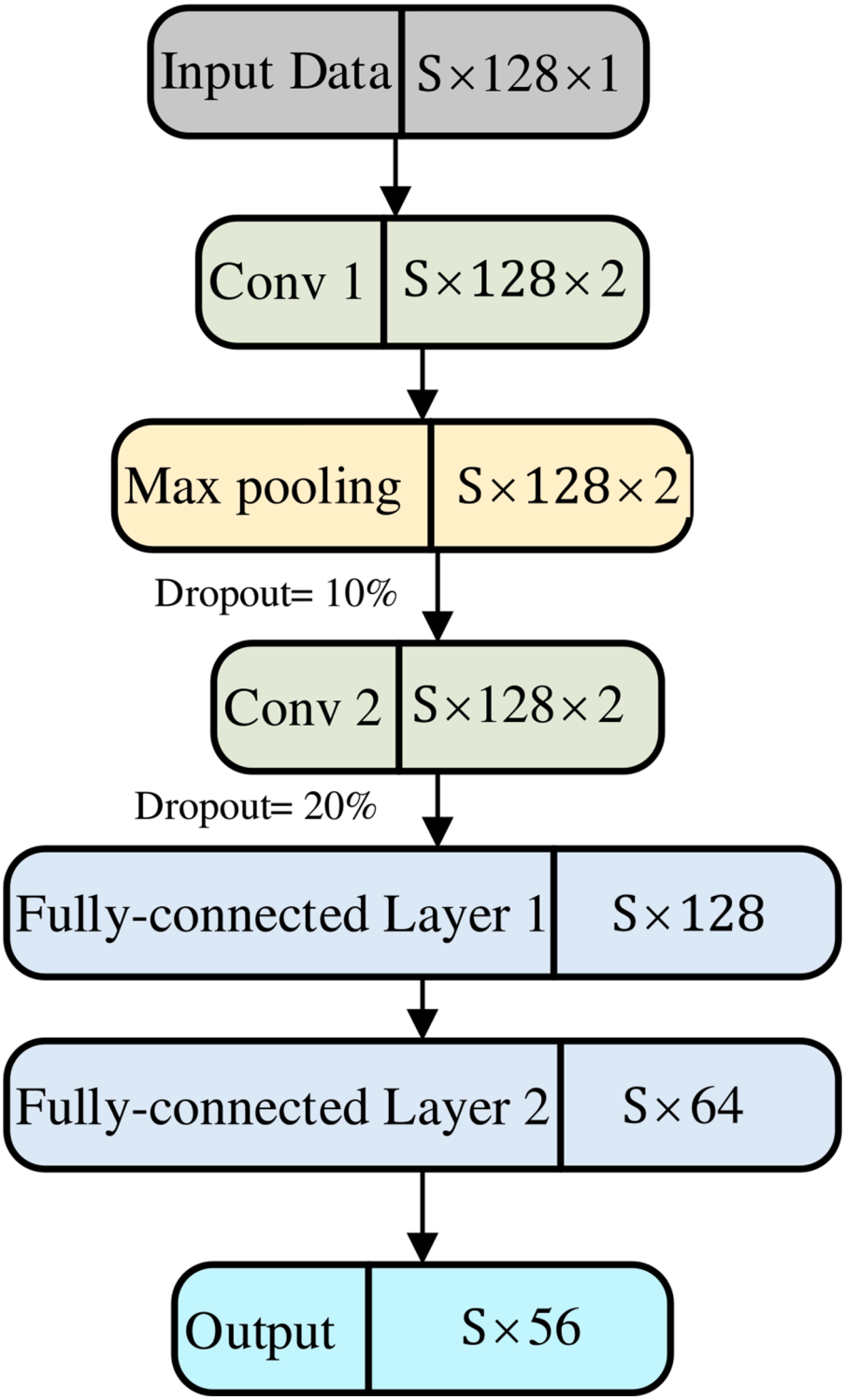

Fig. 5. Structure of designed adaptive 1D-CNN.

adaptive 1D-CNN in the predictive control system of SVCs aiming to mitigate the undesirable flicker impacts is analyzed and compared with, i) the wind farm system connected to the upstream grid without reactive power compensators such as SVC; ii) the wind farm system connected to the SVC with a conventional control system. In this case, the capacitance of the SVC is chosen based on the instantaneous variation of the reactive power at this moment. Thereby, it can be not compensated completely; iii) The wind farm

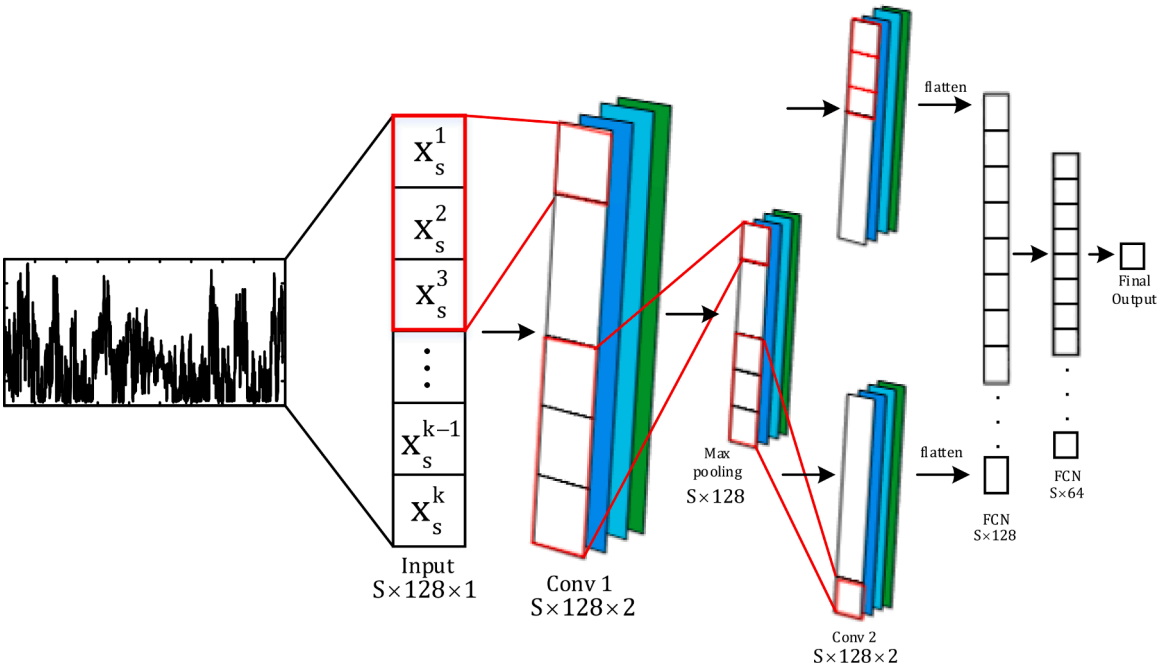

Fig. 6. Structure of the designed 1D-CNN for the reactive power forecasting of the wind farm.

system connected to the SVC with the proposed adaptive deep learning-based control system. It is noticeable that the CNN-based controller causes far smaller total reactive power than the wind farm connected with conventional SVC and without SVC.

The forecasting engines for the extremely short time period have been implemented in the TensorFlow and further process in MATLAB software. Approximately 70% of the actual data is devoted to the training process and the rest of the actual data has been considered for testing the performance. It is noticeable the CNN-based controller causes far smaller total reactive power than wind farms connected with conventional SVC and without SVC.

5.1. Description of the actual data

In this paper, to mimic a realistic case study, a set of actual data is collected from a real wind farm located in a city in the north of Iran, Manjil (coordinates: 36°44′18.1″ N 49°23′51.5″ E). The wind farm in Manjil consists of 174 wind turbines. About 66 wind generators are squirrel cage induction machines ($P_{nominal}$ = 330, 500, 550kW), while a large share of wind generators (108 wind generators) are wound rotor induction machines ($P_{nominal}$ = 660kW).

The studies are related to records gathered from the substation which is connected to the squirrel cage induction generators.

Turbines are connected to dedicated transformers with ratings 2000 kVA, 1250 kVA, and 630 kVA, 20 kV/ 690 V, Y/Δ, and then they are connected to a medium voltage network via switching substations. The short circuit power at PCC point is 500 MVA. Figure 7 displays the schematic of the wind farms and PCC that was used to collect the actual data. Dataset is recorded at the PCC in an interval within 10 s with sampling time 128 μs. In total there are 327 separate 10 s data records which are gathered in different time and operation conditions of the wind farm. Table 2 displays the details of the 10 s records from the 550 kW wind turbines.

The active and reactive power was calculated based on the window involving a full-cycle of a sample, which updates every half-cycle [24,25]. Eqs. (22 and 23) are realizing this method for the 128 μs sampling time where 156 samples exist in the 50 Hz cycle.

$$p_n = \frac{1}{156}\sum_{k=78(n-1)}^{78(n+1)} v_k.i_k \tag{22}$$

$$Q_n = \frac{1}{156}\sum_{k=78(n-1)}^{78(n+1)} v_{k-39}.i_k \tag{23}$$

where n=1,2,…,1000 and k=1,2,…,78,125

Eqs. (22) and (23) converts the v and i signals with the 128 μs sampling time to active and reactive powers time series (each sampling recorded at each 0.01 s). Thus, an adaptive 1D-CNN based forecasting engine, predicts a half-cycle ahead of the time series and the database total length is equal to 327,000 (327*1000) samples.

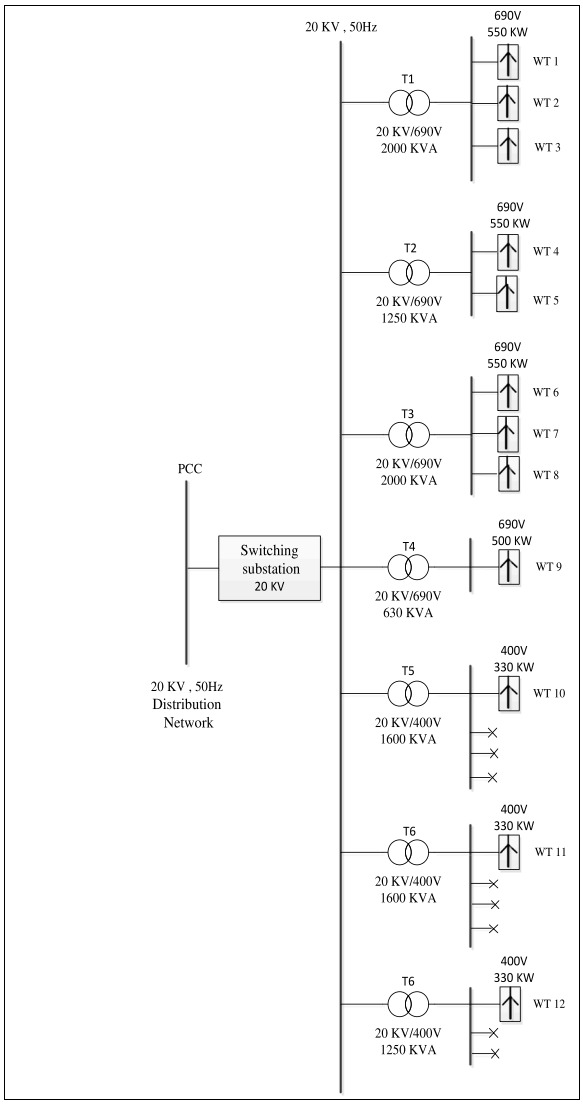

Fig. 7. Schematic of the studied substation of Manjil, Iran network

Table 2
Details of the substation 10 s records.

Date	Time of first record	Time of final record	Number of 3-phase records
2015/06/09	11:23	11:40	10
2015/06/09	23:51	23:58	10
2015/06/10	17:26	17:45	10
2015/06/11	01:13	01:25	10
2015/06/11	04:31	04:47	10
2015/06/11	12:06	12:15	10
2015/06/11	21:16	21:29	10
2015/06/12	08:42	08:55	10
2015/06/12	17:38	17:55	10
2015/06/13	10:28	10:52	10
2015/06/13	14:54	15:11	9

5.2. Discussion on results: Extremely short-term reactive power of wind farms forecasting

The performance of the proposed adaptive 1D-CNN is compared with:

1- Enhanced 2D-CNN with one 2D-convloutional layer, one pooling, and two fully-connected layers [4].
2- Conventional 2D-CNN with similar structure with improved CNN.
3- Conventional 1D-CNN with similar structure with the proposed adaptive 1D-CNN
4- Feedforward neural network (FFNN) with one input layer (86 neurons), two hidden layers which connected in the hidden layer (256 neurons, 128 neurons), and one output layer with one neuron.

The proposed method is compared with these methods in terms of accuracy and computational time. In a real-time control system, computational complexity is a key factor. To provide a comprehensive comparison in terms of accuracy, four different metrics including mean average percentage error (E^{MAPE}), mean absolute error (E^{MAE}), root mean square (E^{RMSE}), and normalized root mean square error (E^{NRMSE}):

$$E^{MAPE} = \sum_{t=1}^{M} \frac{100}{M} \left| \frac{\widehat{Q}_{WT}^{t} - Q_{WT}^{t}}{Q_{WT}^{t}} \right| \tag{24}$$

$$E^{MAE} = \sum_{t=1}^{M} \frac{1}{M} \left| \widehat{Q}_{WT}^{t} - Q_{WT}^{t} \right| \tag{25}$$

$$E^{RMSE} = \sqrt{\frac{1}{M} \sum_{t=1}^{M} \left(\widehat{Q}_{WT}^{t} - Q_{WT}^{t} \right)^2} \tag{26}$$

$$E^{NRMSE} = \frac{1}{Q_{WT}^{max}} \sqrt{\frac{1}{M} \sum_{t=1}^{M} \left(\widehat{Q}_{WT}^{t} - Q_{WT}^{t} \right)^2} \tag{27}$$

where M, $\widehat{Q}_{WT}^{t}$, and Q_{WT}^{t} represents the total number of test data, predicted reactive power at t time interaval, and actual reactive power at t time interval, respectively.

Table 3 compares the results of the proposed adaptive 1D-CNN structure with other methods based on the forecasting error metrics. According to E^{MAE} metric, as an example, the proposed adaptive 1D-CNN method reduces the error obtained by the enhanced 2D-CNN, 2D-CNN, 1D-CNN, and FFNN approximately 6.36%, 42.65%, 73.82%, and 90.00%, respectively.

In terms of computational complexity, the performance time of the different networks is given in Table 4. To this end, we repeated the testing performance 500 times and then, the average and maximum performance time is depicted in Table 4. As can be seen, FFNN is the fastest method in extremely short-term forecasting, while the accuracy of FFNN is not acceptable. The testing time of adaptive 1D-CNN and 1D-CNN is the same, because, the main difference in these two methods is related to the training process. The training time of the adaptive 1D-CNN is about 32 min, while the training time of conventional 1D-CNN is about 1hr and 12 min. The maximum testing time of enhanced 2D-CNN and conventional 2D-CNN confirms that these two methods are more or less inappropriate for the real-time control system of SVC connected to the wind farms.

5.3. Discussion on results: flicker mitigation

In this subsection, the results obtained in the three mentioned cases are discussed and compared based on three different measures including instantaneous flicker sensation (mean and maximum values), short-term flicker indicator (P_{st}), and instantaneous reactive power variations.

Fig. 8 illustrates the instantaneous reactive power for a sample of actual recorded data, as an example, in three different cases. Indeed, Fig. 8(a) illustrates one of the reactive power records of the wind farm as a snapshot of the input signal that is used for the proposed adaptive 1D-CNN method. The reactive power behavior in the presented predictive control system is smoother than cases

Table 3
Error obtained by Extremely short-term prediction results based different deep and shallow methods.

Methods	E^{NRMSE}	$E^{RMSE}(VAR)$	$E^{MAE}(VAR)$	$E^{MAPE}(\%)$
Adaptive 1D-CNN	0.0102	995.48	869.52	0.2914
Enhanced 2D-CNN	0.0160	1194.26	928.64	0.3068
2D-CNN	0.042	3140.78	1516.11	0.4875
1D-CNN	0.0540	4569.32	3321.74	1.0575
FFNN	0.1005	9945.50	8695.85	5.0120

Table 4
Error obtained by Extremely short-term prediction results based different deep and shallow methods.

Methods	Adaptive 1D-CNN	Enhanced 2D-CNN	2D-CNN	1D-CNN	FFNN
Mean Performance Time (ms)	8.75	9.82	15.42	8.75	2.42
Max Performance Time (ms)	9.12	11.2	17.52	9.12	3.86

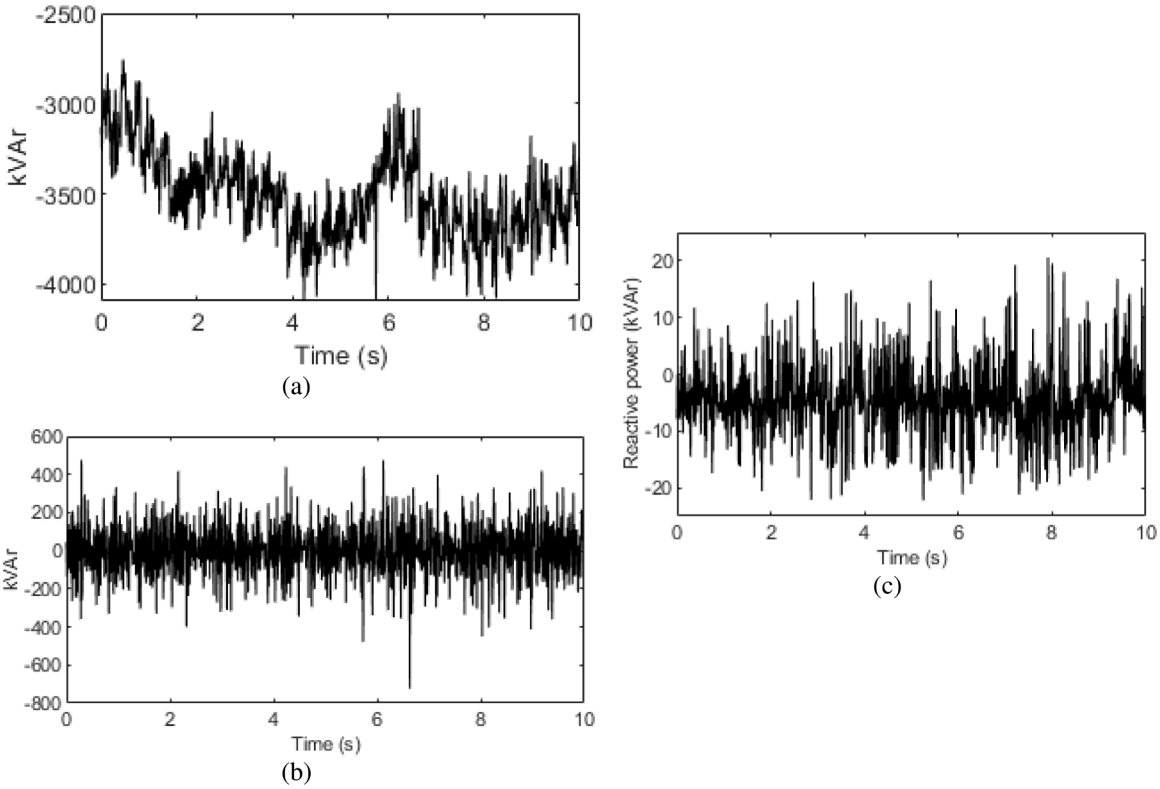

Fig. 8. Reactive power variations (a) Without SVC, (b) SVC with conventional control system, (c) SVC with predictive control system

with conventional SVC and without SVC. From Fig. 8(c), the fluctuation of the instantaneous reactive power with high negative magnitude demonstrates the necessity of reactive power compensation in large-scale wind farms.

Flicker sensation values can be suitable measures to access three different cases including an adaptive deep learning based control system. Flicker sensation compute based on IEC standard (IEC 868) and the network short-circuit is 50 MVA.

Fig. 9 compares the performance of the proposed adaptive CNN-based control system with cases I & II based on flicker sensation in one specific record. The superiority of the proposed 1D-CNN based controller is obvious by the least flicker sensation values of the actual record throughout the period displayed. The instantaneous flicker sensation in Cases II and I even reach values higher than 2, which reveals that voltage flicker cannot be properly compensated.

To extensively compare the three cases, the results obtained by 10 different actual records are accessed. Table 5 compares the mean values of instantaneous flicker among all three cases for 10 different actual records. The proposed 1D-CNN network based predictive controller has the lowest mean flicker sensation in comparison with the other two cases. For instance, in record 9, the predictive controller has improved the wind farm with a conventional control system and without the reactive power compensation device more than 99.57% and 99.80%, respectively. The inferiority and superiority of Cases I & III are pretty obvious based on Table 5.

Table 6 displays the maximum values of instantaneous flicker sensation in order to compare the performance of all cases. Similar to Table 5, the superiority of the adaptive 1D-CNN based control system is clear in Table 6. For instance, in a case without reactive power compensation device installation, the Record 6 has the worst values in terms of mean value of flicker sensation (9.1555), while the deep neural network based control system is improved by 84.54%. The worst condition in Case II is related to record number 9. In this record, the maximum of instantaneous flicker sensation of Case II is 4.5028, while the proposed control system has reduced this value to 0.0050.

Table 7 depicts the P_{st} values in cases I, II, and III. From this table, it is obvious that the P_{st} values are far higher than the proposed adaptive 1D-CNN based control system. In better words, from the P_{st} point of view, the superiority of the proposed adaptive deep based network is obvious. For instance, in record number 7, approximately 99.83% and 99.49% improvement in the P_{st} values can be seen in

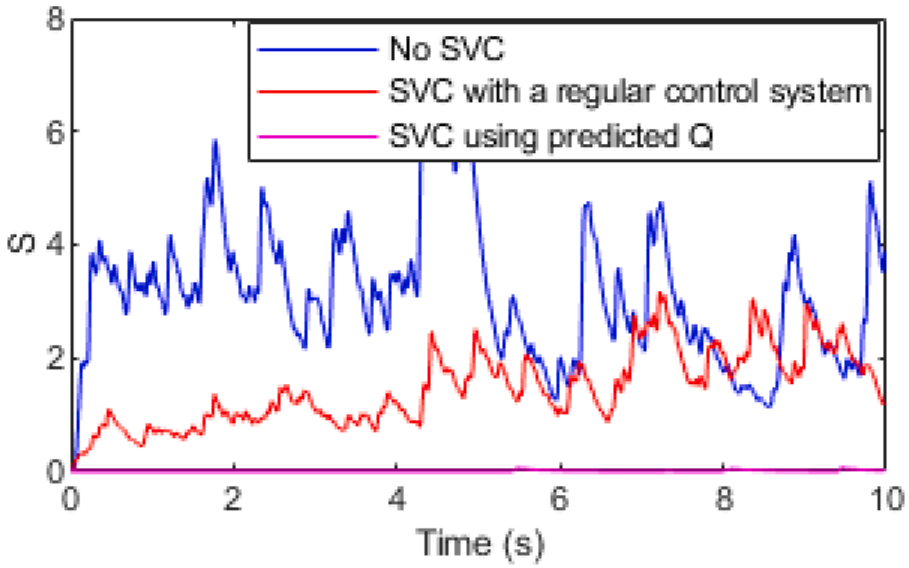

Fig. 9. Comparison of the predictive control for SVC with the conventional control system of SVC and the wind farm without SVC based on the instantaneous flicker sensation.

Table 5
Results of cases I, II, II In terms of mean value of instantaneous flicker sensation.

SVC with proposed predictive control system	SVC with conventional control system	Without SVC	Mean value of instantaneous flicker
0.0062	1.4626	3.1608	Record 1
0.0063	0.7321	3.4721	Record 2
0.0112	0.7621	2.9140	Record 3
0.0087	0.9976	3.0782	Record 4
0.0033	1.0333	3.1541	Record 5
0.120	1.1947	3.2899	Record 6
0.0014	1.1286	3.1295	Record 7
0.0026	1.2476	2.9780	Record 8
0.0014	1.6441	3.1465	Record 9
0.0010	1.1911	3.0444	Record 10

Table 6
Results of Cases I, II, II In terms of MAX value of Flicker sensation.

Max value of instantaneous flicker	Without SVC	SVC with conventional control system	SVC with proposed predictive control system
Record 1	7.0179	3.1832	0.0574
Record 2	7.1557	1.6566	0.0943
Record 3	6.3882	1.4407	0.1625
Record 4	7.1595	1.9278	0.0730
Record 5	7.6469	1.9260	0.0519
Record 6	9.1555	2.4758	0.1474
Record 7	6.8771	2.2164	0.0113
Record 8	8.3746	2.3097	0.0510
Record 9	6.2300	4.5028	0.0050
Record 10	6.34364	2.4948	0.0058

the comparison between the proposed predictive control system rather than Cases I and II, respectively.

Conclusions and future work

In terms of economic and technical considerations, SVC is the most preferable to install within wind farms to mitigate flicker emissions. However, SVC suffers from an inherent time delay problem, which adversely affects the performance of reactive power compensation in the wind farms. To address this problem, deep learning based predictive controller is proposed in this study. An adaptive 1D-CNN based structure is designed as an extreme short-term forecasting engine and applied as an additional block to compensate for the inherent delay by SVC. The designed adaptive 1D-CNN has the capability to learn volatile and complex features

Table 7
Results of Cases I, II, II In terms of P_{st} values.

P_{st}	Without SVC	SVC with conventional control system	SVC with proposed predictive control system
Record 1	1.6030	1.1016	0.1167
Record 2	1.5734	0.7349	0.1272
Record 3	1.5734	0.7369	0.1646
Record 4	1.6029	0.8558	0.1300
Record 5	1.6029	0.8533	0.0839
Record 6	1.6692	0.9766	0.1608
Record 7	1.6040	0.9247	0.0488
Record 8	1.6041	0.9499	0.0806
Record 9	1.5372	1.2493	0.0410
Record 10	1.5611	0.9420	0.0348

directly from reactive power data within a half-cycle time resolution. As the extremely short-term forecasting engine, the proposed method is compared with improved 2D-CNN, standard 2D-CNN, standard 1D-CNN, and FFNN. The results demonstrate the superiority of the proposed method based on four different accuracy metrics and computational complexity, more than 12% improvement in terms of accuracy, and lower computational time in comparison with deep CNN-based networks. Furthermore, the proposed predictive control system for SVC is compared with SVC with a conventional control system and the wind farm without reactive power compensation devices in terms of flicker emission reduction and reactive power compensation. The results indicate that the adaptive deep learning based control system has led to more than 99% improvement compared to the SVC with a conventional control system and without the reactive power compensation based on the mean/max instantaneous flicker and more than 99% based on Pst. Numerical investigation validated the effectiveness and superiority of the proposed control system. In the real-time control system, one major challenge would be data interruption. Thus, in our future work, we would focus on developing a predictive block to be robust in the data interruption conditions.

CRediT authorship contribution statement

Haidar Samet: Conceptualization, Methodology, Project administration, Supervision, Writing – review & editing, Data curation. **Saeedeh Ketabipour:** Methodology, Software, Writing – original draft, Visualization, Validation, Formal analysis, Investigation. **Shahabodin Afrasiabi:** Methodology, Software, Writing – original draft, Visualization, Validation, Formal analysis. **Mousa Afrasiabi:** Methodology, Software, Writing – original draft, Visualization, Validation, Formal analysis. **Mohammad Mohammadi:** Resources, Supervision.

Declaration of Competing Interest

None.

References

[1] Abedinia O, Bagheri M, Naderi MS, Ghadimi N. A new combinatory approach for wind power forecasting. IEEE Syst J 2020:1–12.
[2] Samet H, Bagheri AA. Enhancement of SVC performance in flicker mitigation of wind farms. IET Gener, Transm Distrib 2017;11(15):3823–34.
[3] "SVCs for voltage stabilization in grid with heavy wind power penetration", ABB, [Online]: Availabale: https://library.e.abb.com/public/16200070bd7ac76c8325773b0028ade7/A02-0204%20E%20LR.pdf.
[4] Samet H, Ketabipoor S, Afrasiabi M, Afrasiabi S, Mohammadi M. Deep learning forecaster based controller for SVC: wind farm flicker mitigation. IEEE Trans Ind Inf 2020:1.
[5] Sharma SK, Chandra A, Saad M, Lefebvre S, Asber D, Lenoir L. Voltage flicker mitigation employing smart loads with high penetration of renewable energy in distribution systems. IEEE Trans Sustain Energy 2017;8(1):414–24.
[6] Tao S, Zhe C, Blaabjerg F. Flicker study on variable speed wind turbines with doubly fed induction generators. IEEE Trans Energy Convers 2005;20(4):896–905.
[7] Soliman MA, Hasanien HM, Azazi HZ, El-Kholy EE, Mahmoud SA. An adaptive fuzzy logic control strategy for performance enhancement of a grid-connected PMSG-based wind turbine. IEEE Trans Ind Inf 2019;15(6):3163–73.
[8] Samet H, Jarrahi MA. A comparison between SVC and STATCOM in flicker mitigation of electric arc furnace using practical recorded data. In: 2015 30th International Power System Conference (PSC); 2015. p. 300–4.
[9] Samet H, Reisi M, Marzbani F. Evaluation of neural network-based methodologies for wind speed forecasting. Comput Electr Eng 2019;78:356–72.
[10] Afrasiabi M, Mohammadi M, Rastegar M, Afrasiabi S. Advanced deep learning approach for probabilistic wind speed forecasting. IEEE Trans Ind Inf 2021;17(1):720–7.
[11] Kreutz M, et al. Machine learning-based icing prediction on wind turbines. Procedia CIRP 2019;81:423–8.
[12] Howland MF, Dabiri JO. Wind farm modeling with interpretable physics-informed machine learning. Energies 2019;12(14):2716.
[13] Ansari M, Latify MA, Yousefi GR. GenCo's mid-term optimal operation analysis: interaction of wind farm, gas turbine, and energy storage systems in electricity and natural gas markets. IET Gener, Transm Distrib 2019;13(12):2328–38.
[14] Aguilar S, Santos DRd, Souza RC. Long-term forecasting of wind speed in Brazil using GAS modelling. In: 7th International Conference on Renewable Energy Research and Applications (ICRERA); 2018. p. 727–31.
[15] Afrasiabi M, Mohammadi M, Rastegar M, Stankovic L, Afrasiabi S, Khazaei M. Deep-based conditional probability density function forecasting of residential loads. IEEE Trans Smart Grid 2020;11(4):3646–57.
[16] Lu L, Zhang J, Jing X, Khan MK, Alghathbar K. Dynamic weighted discrimination power analysis in DCT domain for face and palmprint recognition. In: 2010 International Conference on Information and Communication Technology Convergence (ICTC); 2010. p. 467–71.
[17] Leng L, Li M, Kim C, Bi X. Dual-source discrimination power analysis for multi-instance contactless palmprint recognition. Multim Tools Appl 2017;76(1):333–54.

[18] Afrasiabi S, Afrasiabi M, Parang B, Mohammadi M. Integration of accelerated deep neural network into power transformer differential protection. IEEE Trans Ind Inf 2020;16(2):865–76.
[19] Zhang S, Zhang S, Wang B, Habetler TG. Deep learning algorithms for bearing fault diagnostics—a comprehensive review. IEEE Access 2020;8:29857–81.
[20] Miller TJE. Reactive power control in electric systems. Wiley; 1982.
[21] Afrasiabi M, Mohammadi M, Rastegar M, Kargarian A. Multi-agent microgrid energy management based on deep learning forecaster. Energy 2019;186:115873.
[22] Afrasiabi M, Mohammadi M, Rastegar M, Kargarian A. Probabilistic deep neural network price forecasting based on residential load and wind speed predictions. IET Renew Power Gener 2019;13(11):1840–8.
[23] Tieleman T, Hinton G. Lecture 6.5-rmsprop: Divide the gradient by a running average of its recent magnitude. COURSERA: Neural Netw Mach Learn 2012;4(2):26–31.
[24] Samet H. Evaluation of digital metering methods used in protection and reactive power compensation of micro-grids. Renewable Sustain Energy Rev 2016;62:260–79.
[25] Samet H, Masoudipour I, Parniani M. New reactive power calculation method for electric arc furnaces. Measurement 2016;81:251–63.

Haidar Samet received the Ph.D. degree in electrical engineering from Isfahan University of Technology, in 2008. He is currently a Professor with School of Electrical and Computer Engineering, Shiraz University. His-major research interests include protection of power systems, electric arc furnaces, and application of time series in power systems.

Saeedeh Ketabipour received the B.*Sc*. and M.*Sc*. degrees in electrical power engineering in 2010 and 2013, respectively, from Khuzestan Water and Electricity Industry Research and Educational Center, Ahvaz, Iran, and Islamic Azad University of Khomeini Shahr, Isfahan, Iran. Her main research interest is the power quality of power systems.

Shahabodin Afrasiabi received the B.*Sc*. degree from Semnan University, Semnan, Iran, in 2014, and his M.*Sc*. degree from the Shahid Chamran University of Ahvaz, Ahvaz, Iran, in 2017. His-research interests include power system dynamic analysis, machine learning, fault diagnosis, energy management, electric machine design, state estimation, time series forecasting and power system probabilistic analysis.

Mousa Afrasiabi received the B.*Sc*. degree from University of Guilan, Rasht, Iran, in 2008, his M.*Sc*. degree from the K.N. Toosi University of Technology, Tehran, Iran, in 2011, and his Ph.D from the Shiraz University, Shiraz, Iran. in electrical power engineering. His-research interests include energy management, time series forecasting, machine learning, and power system probabilistic analysis.

Mohammad Mohammadi received the B.*Sc*. degree from Shiraz University, Shiraz, Iran, in 2000, and the M.*Sc*. and Ph.D. degrees from the Amirkabir University of Technology, Tehran, Iran, in 2002 and 2008, respectively. His-research interests include power system probabilistic analysis, power system security assessment, machine learning, and power system dynamic analysis.